IEICE TRANS. FUNDAMENTALS, VOL.E107–A, NO.6 JUNE 2024

LETTER

Performance of the Typical User in RIS-Assisted Indoor Ultra Dense Networks

Sinh Cong LAM[†a)], ***Member***, **Bach Hung LUU**[†], ***and*** **Kumbesan SANDRASEGARAN**[††], ***Nonmembers***

SUMMARY Cooperative Communication is one of the most effective techniques to improve the desired signal quality of the typical user. This paper studies an indoor cellular network system that deploys the Reconfigurable Intelligent Surfaces (RIS) at the position of BSs to enable the cooperative features. To evaluate the network performance, the coverage probability expression of the typical user in the indoor wireless environment with presence of walls and effects of Rayleigh fading is derived. The analytical results shows that the RIS-assisted system outperforms the regular one in terms of coverage probability.

key words: *cooperative communication, reconfigurable intelligent surfaces, coverage probability, ultra dense networks, indoor*

1. Introduction

The exponential increase in the number of users and high speed data requirements is promoting the employment of advanced techniques in the cellular network systems. One of the most potential techniques is cooperative communication that utilizes more than one Base Stations (BSs) to serve the active user [1]. Recently, Reconfigurable Intelligent Surfaces (RIS) was introduced to enable the main features of cooperative communication but with lower installation cost [2]. The feasibility of RIS deployment and design in the ultra dense network has attracted a huge amount of works in both academic and industrial areas such as [3], [4].

Although the benefits of RIS have been conducted in various research, the location of RIS elements in the network needs more works. In [5], the RISs are uniformly distributed in 2-D Coordinate System so that there exists the Light-of-Sight (LoS) between the RIS and target user. In [6], the RISs are located at the middle point of the blockages whose positions follows the Poisson Point Process (PPP). The binomial point process and independent PPP were also utilized to model the position of RIS in [7] and [8], respectively. With assumption of random distribution, the authors in [9] proposed an algorithm to select the optimal RIS.

Although the mentioned papers illustrated that discussed location of RISs can improve the network performance, utilization of random process to locate the RISs may be unfeasible due to the complexity of transmission condition. In the indoor environment with various obstacles such as walls and furniture, there may not have enough free space to install both small cell stations and RISs. In addition, since RISs are usually the passive devices that only reflect the signal from the transmitter without signaling messages, the selection of optimal RIS is a big challenge. In this paper, an other potential location of RISs is discussed with the criteria of simplicity and installation cost. Specifically, RISs are located on the same tower with the BSs. Thus, the typical user can be served by the nearest BS and the RIS that is located at the position of the second nearest BS. To prove the benefits of the model, this paper adopts the recent developed path loss model [10], which considers the walls' density and properties, to analyze the user coverage probability.

2. System Model

In this paper, we studies an indoor millimeter wave cellular network with RIS assistance as illustrated in Fig. 1. Particularly, each BS whose position follows the the Spatial Poisson Point Process (PPP) is equipped antenna as the primary transmitter and RIS elements to assist the communication between the user and BS in the adjacent cell. Thus, the density of the BSs is the same as that of the RISs which is λ (BS/m^2). Without loss of generality, it is assumed that the typical user is located at the origin and receives signal from the nearest BS. In addition, this user also receives the signal from the RIS which has the same location with the second nearest BS. It is noted that if the link between the typical user and its nearest BS is blocked, the link between the nearest RIS and the user is also blocked.

Let $r^{(k)}$ as the distance from the typical user to BS k;

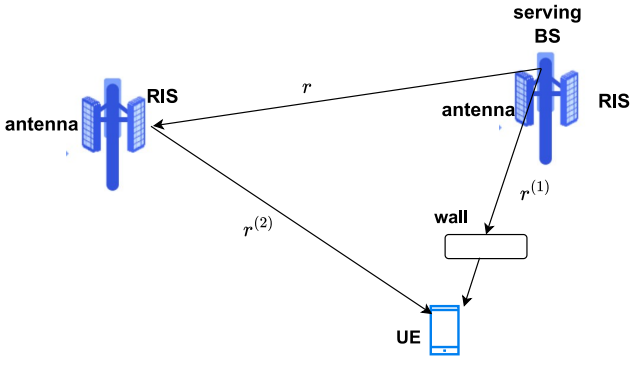

Fig. 1 System model.

Manuscript received January 4, 2024.
Manuscript revised February 17, 2024.
Manuscript publicized March 6, 2024.

[†]The authors are with the Faculty of Electronics and Telecommunication, VNU University of Engineering and Technology, Vietnam.
[††]The author is with Bangkok University, Thailand.
a) E-mail: congls@vnu.edu.vn

DOI: 10.1587/transfun.2024EAL2001

$\phi^{(k)}$ $\left(0 \le \phi^{(k)} \le 2\pi\right)$ as the angle between the horizontal axis of the Cartesian coordinate system and the vector that starts from the origin and ends at the position of BS k. Thus, the position of BS k is $\left(r^{(k)} \cos \phi^{(k)}, r^{(k)} \sin \phi^{(k)}\right)$. As presented in the literature [11], the joint Probability Density Function (PDF) of the distance from the typical user to its nearest BS $r^{(1)}$, i.e. primary serving BS, and second nearest BS $r^{(2)}$, i.e. the RIS of this user, is computed as follows:

1. The PDF of the distance from the typical user to its nearest BS $r^{(1)}$ is

$$f_1\left(r^{(1)}\right) = 2\pi\lambda r^{(1)} \exp\left(-\pi\lambda\left[r^{(1)}\right]^2\right) \tag{1}$$

2. The probability that there is no BS in area A is $\exp(-\lambda A)$. Hence, the probability that there is no point between $r^{(1)}$ to $r^{(2)}$ is

$$P_{12}(0) = \exp\left(-\pi\lambda\left(\left[r^{(2)}\right]^2 - \left[r^{(1)}\right]^2\right)\right)$$

3. The PDF of $r^{(2)}$ under the condition of $r^{(1)}$ is $f\left(r^{(2)}\middle|r^{(1)}\right) =$

$$2\pi\lambda r^{(2)} \exp\left(-\pi\lambda\left(\left[r^{(2)}\right]^2 - \left[r^{(1)}\right]^2\right)\right)$$

4. Consequently, the joint PDF of $r^{(1)}$ and $r^{(2)}$ is $f_{12}\left(r^{(1)}, r^{(2)}\right)$

$$\begin{aligned} &= f_{12}\left(r^{(2)}\middle|r^{(1)}\right) f_1\left(r^{(1)}\right) \\ &= (2\pi\lambda)^2 r^{(1)} r^{(2)} \exp\left(-\pi\lambda\left[r^{(2)}\right]^2\right) \end{aligned} \tag{2}$$

In addition, the distance between the serving BS and RIS of the typical user

$$r = \sqrt{\left[r^{(1)}\right]^2 + \left[r^{(2)}\right]^2 - 2r^{(1)}r^{(2)}\cos\left[\phi^{(1)} - \phi^{(2)}\right]}$$

Since all BSs are uniformly distributed, $\phi^{(1)}$ and $\phi^{(2)}$ are uniform random variables (RVs) in a range of $[0, 2\pi]$. Letting $\Phi = |\phi^{(1)} - \phi^{(2)}|$, then the PDF of Φ is

$$f_\Phi(\Phi) = \frac{2\pi - \Phi}{2\pi^2}; \quad 0 \le \Phi \le 2\pi \tag{3}$$

2.1 Large-Scale Fading and Small-Scale Fading

The indoor environment is usually constructed by walls whose position, density and length are different between scenarios. In this paper, it is assumed that the walls has a average length of L and a distribution of a Spatial PPP with density λ_w. Thus, the average number of walls between the transmitter and receiver at a distance of r is

$$W(r) = \frac{2\lambda_w L}{\pi} r = \beta r \quad \text{where} \quad \beta = \frac{2\lambda_w L}{\pi} \tag{4}$$

In addition, the probability of LoS and nLoS scenarios are respectively [12]

$$p_l(r) = \exp(-\beta r) \text{ and } p_n(r) = 1 - \exp(-\beta r) \tag{5}$$

The main difference between the signal transmission in the LoS and nLoS scenarios is that the signal in the nLoS scenario is blocked and attenuated by the walls. Let ω as the induction ability of a single wall, the received signal power at a distance of r over LoS and nLoS scenarios with an unit transmission power are computed as [10]

$$L(r) = \begin{cases} L_l(r) = r^{-\alpha} & \text{in the case of LoS} \\ L_n(r) = \omega^{\beta r} r^{-\alpha} & \text{in the case of nLoS} \end{cases} \tag{6}$$

where α is the path loss parameter. It is reminded that Ref. [10] defines ω as the attenuation of each wall. This definition can deduce that a higher value of ω reflects a higher attenuation and consequently a lower received signal power. However, Eq. (6) shows that the received signal power increases with the value of ω. Thus, this paper calls ω as the induction ability of a single wall to reflect the exact meaning of this parameter in the path loss model.

Besides, the path loss, i.e. large-scale fading, the signal is usually affected by the multi-path effects whose aptitude is modeled as the Rayleigh RV. Thus, the power gain of the small-scale fading has an exponential distribution.

2.2 Downlink SNR

With the assistance from RIS, the typical user simultaneously receives signals from the serving BS and RIS. To achieve a high performance, the typical user utilizes the Maximum Ratio Combing technique to combine two version of the desired signals. Specially,

- The received signal power of the typical user from the serving BS is

$$S_b = P g^{(1)} L\left(r^{(1)}\right) \tag{7}$$

  where P is the BS transmission power; $g^{(1)}$ is the channel power gain between this BS and the typical user.
- The received signal of the typical user from the RIS is

$$S_r = P g^{(12)} L(r)\, g^{(2)} L\left(r^{(2)}\right) \tag{8}$$

  where $P g^{(12)} L(r)$ is the signal power that the RIS receives from the serving BS; $g^{(2)}$ is the channel power gain between the RIS and the typical user.
- Hence, the total received power at the typical user is

$$S = P g^{(1)} L\left(r^{(1)}\right) + P L(r)\, g^{(12)} g^{(2)} L\left(r^{(2)}\right)$$

With assumption that $g^{(1)}$ has an exponential distribution with a PDF of $f(g) = \exp(-g)$, $P g^{(1)} L(r^{(1)})$ is also a exponential RV with a mean of $P L(r^{(1)})$. In addition, the $g^{(12)} g^{(2)}$ is the product of two exponential RVs with mean 1. Thus, it can be approximated by a single normalized Gamma RV

with the shape parameter k and the scale parameter θ ($k\theta = 1, \theta > 1$). Consequently, $PL(r)\, g^{(12)} g^{(2)} L\left(r^{(2)}\right)$ is a gamma RV with a shape of k and a scale of $\Theta_{12} = \theta PL(r)\, L\left(r^{(2)}\right)$.

Hence, $S = Pg^{(1)} L(r^{(1)}) + PL(r)\, g^{(12)} g^{(2)} L\left(r^{(2)}\right)$ is the sum of two gamma RVs. By the meaning of Welch-Satterthwaite approximation [13], S can be approximated by $P\mathcal{L}Y$ where Y is a normalized Gamma RV with the shape of

$$p = \frac{\left[L(r^{(1)}) + L(r)\, L\left(r^{(2)}\right)\right]^2}{\left[L(r^{(1)})\right]^2 + \theta\left[L(r)\, L\left(r^{(2)}\right)\right]^2} \tag{9}$$

where $\mathcal{L} = L\left(r^{(1)}\right) + L\left(r^{(2)}\right) L(r)$. Thus, the definition of CDF of S is presented as follows

$$F_S(x) = \int_0^x \frac{p^p u^{p-1}}{\Gamma(p)} \exp(-pu)\, du \tag{10}$$

By following a change of variable $t = (pu)^p$, the CDF of S is re-written as follows

$$F_S(x) = \frac{1}{\Gamma(p+1)} \int_0^{(px)^p} \exp\left(-t^{\frac{1}{p}}\right) dt \tag{11}$$

Utilizing the result in the literature [14] which concludes that

$$\frac{1}{\Gamma(1+1/v)} \int_0^z \exp(-t^v)\, dt < \left[1 - \exp(-\beta z^v)\right]^{1/v}$$

with $\beta = [\Gamma(1+1/v)]^{-p}$ for $v = 1/p$, $z = (px)^p$, we obtain the tightly approximation of $F_S(x)$ as follows

$$F_S(x) \approx \left[1 - \exp\left(-\Upsilon_p x\right)\right]^p \tag{12}$$

where $\Upsilon_p = p\left[\Gamma(1+p)\right]^{-1/p}$. By apply the Newton's generalized binomial theorem, the tightly upper bound of CDF of S is approximated as follows

$$F_S(x) \approx \sum_{m=0}^{M} \rho(p,m)(-1)^m \exp\left(-m\Upsilon_p x\right) \tag{13}$$

where $\rho(p,m) = \frac{p(p-1)\ldots(p-m+1)}{m!}$; M is an integer. M is selected so that the approximation is convergence.

Consequently, the downlink Signal-to-Noise Ratio at the typical user with Gaussian power of σ^2 is given by

$$SNR = \frac{P\mathcal{L}Y}{\sigma^2} \tag{14}$$

3. Coverage Probability

To examine the downlink performance of the typical user in the cellular network, the coverage probability is widely used as the key metric, which is defined as

$$\mathcal{P} = \mathbb{P}(SNR > T) \tag{15}$$

where SNR is defined in Eq. (14); $\mathbb{P}$ presents the conditional probability. The downlink coverage probability is expanded as follows

$$\mathcal{P} = \mathbb{P}\left(\frac{P\mathcal{L}Y}{\sigma^2} > T\right) \tag{16}$$

Since each path loss comprises of LoS and nLoS scenarios as in Eq. (6),

$$\mathcal{P} = \sum_{u\in\{n,l\}} \sum_{v\in\{n,l\}} \sum_{z\in\{n,l\}} \mathbb{E}\begin{bmatrix} p_u\left(r^{(1)}\right) p_v\left(r^{(2)}\right) p_z(r) \\ \times\mathbb{P}\left(Y > \frac{T}{\gamma\mathcal{L}}\right) \end{bmatrix}$$

where $\gamma = P/\sigma^2$, $\{n,l\}$ correspond to nLoS and LoS, respectively; $\mathbb{E}$ is used to indicate the conditional expectation. Utilizing the approximation of CDF of Y in Eq. (13),

$$\mathcal{P} = \sum_{u\in\{n,l\}} \sum_{v\in\{n,l\}} \sum_{z\in\{n,l\}} \sum_{k=1}^{M} \rho(p,k)(-1)^{m+1} \times\mathbb{E}\begin{bmatrix} p_u\left(r^{(1)}\right) p_v\left(r^{(2)}\right) \\ \times p_z(r) \exp\left(-\frac{mT\Upsilon_m}{\gamma\mathcal{L}}\right) \end{bmatrix}$$

It is noted that $\mathcal{L} = L\left(r^{(1)}\right) + L\left(r^{(2)}\right) L(r)$ and r are the function of the uniform RV θ, $r^{(1)}$ and $r^{(2)}$. In addition, the joint PDF of $r^{(1)}$ and $r^{(2)}$ is presented in Eq. (2). Hence, the downlink coverage probability is obtained by taking the expectation with respects to three RVs ϕ, $r^{(1)}$ and $r^{(2)}$ as

$$\mathcal{P} = \sum_{u\in\{n,l\}} \sum_{v\in\{n,l\}} \sum_{z\in\{n,l\}} \sum_{m=1}^{M} \rho(p,k)(-1)^{m+1} \times \int_0^\infty \int_{r^{(1)}}^\infty \int_0^{2\pi} \begin{bmatrix} p_u\left(r^{(1)}\right) p_v\left(r^{(2)}\right) \\ \times p_z(r) \exp\left(-\frac{mT\Upsilon_m}{\gamma\mathcal{L}}\right) \\ \times f_{12}\left(r^{(1)}, r^{(2)}\right) f_\Phi(\Phi) \end{bmatrix} d\Phi dr^{(2)} dr^{(1)} \tag{17}$$

Equation (17) is the coverage probability expression of the typical user in the proposed system model where $p_u\left(r^{(1)}\right), p_v\left(r^{(2)}\right)$ and $p_z(r)$ with $u, v, z \in \{n,l\}$ are obtained from Eqs. (5) and (6).

4. Simulation and Analysis

In this section, the theoretical analysis of user coverage probability in the system with RIS assistance is verified by Monte Carlo simulation and compared to the coverage probability of the typical user in the system without RIS assistance. The following parameters are adopted in this section

- The wall induction ω varies from 0.1 to 0.8 where $\omega = 1$ corresponds to the case that most of signal power is blocked by the wall.
- The coefficient of Newton's generalized binomial theorem M is high enough so that the approximation is convergence. In our analysis, $M = 10$ is selected.

In Fig. 2, the effects of wall induction ability ω on the user coverage probability is visualized and validated by Monte Carlo simulation. Since ω represents how much the signal power can pass the wall, a higher value of ω means

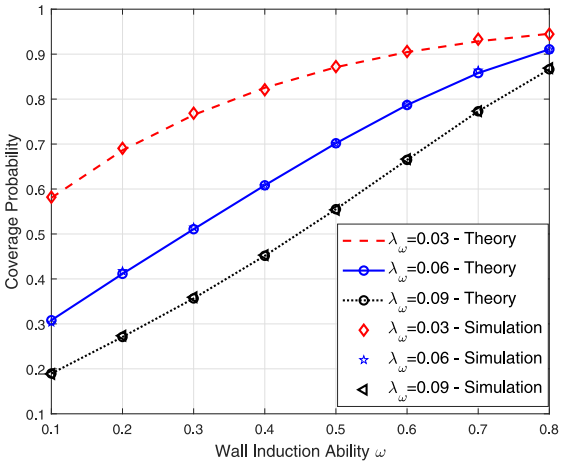

Fig. 2 User coverage probability vs wall induction ability ω.

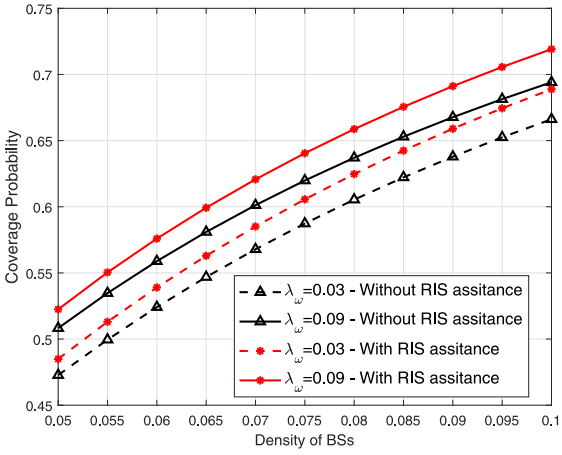

Fig. 3 User coverage probability vs density of BSs.

results in a higher received signal power at the typical user. Thus, the user coverage probability increases with ω.

In addition, a higher number of walls causes a higher probability that the signal is blocked or a higher nLoS probability. In other words, the received signal power and consequently user coverage probability reduces as the density of walls increases. Take the wall induction ability $\omega = 0.2$ for example, the user coverage probability in the case of $\lambda_w = 0.03$ $(wall/m^2)$ is about 0.7 which is 70% higher than another in the case of $\lambda_w = 0.04$ $(wall/m^2)$.

In Fig. 3, the coverage probability of the typical user in the system with RIS assistance and another in the system without RIS assistance is compared as the density of walls and BSs vary. It is noted that the RIS-assisted system allows the typical user to receive signal from both the serving BS and RIS at the position of the second nearest BS of this user. While the typical user in the regular system without RIS only receives signal from the serving BS. Thus, it is reasonable that the typical user in the RIS-assisted system achieves a higher throughput than another in the regular one. Particularly, when $\lambda_w = 0.09$ $(wall/m^2)$, the typical user in the RIS-assisted system achieves a coverage probability of 0.73 if $\lambda = 0.1$ (BS/m^2) which is around 6% higher than another in the system without RIS.

5. Conclusion

This paper studies an indoor cooperative communication system where each BS is equipped with a RIS to reflect the signal from the typical user at the adjacent cell. By this way, the installation cost can be less than the regular RIS-assisted system while the typical user still can receive signal from both RIS and the serving BS. The analytical results in the indoor environment with the presence of walls illustrates that the RIS-assisted system can improve the user coverage probability upto 6%.

References

[1] 3GPP TS 36.300 ver. 15.10.0 Rel. 15, "LTE; Evolved Universal Terrestrial Radio Access (E-UTRA) and Evolved Universal Terrestrial Radio Access Network (E-UTRAN); Overall description," Dec. 2019.

[2] M. Di Renzo, F.H. Danufane, and S. Tretyakov, "Communication models for reconfigurable intelligent surfaces: From surface electromagnetics to wireless networks optimization," Proc. IEEE, vol.110, no.9, pp.1164–1209, 2022.

[3] C. Zhang, Y. Peng, M. Yue, and F. Al-hazemi, "A simple design of reconfigurable intelligent surface-assisted index modulation: Generalized reflected phase modulation," IEICE Trans. Fundamentals, vol.E107-A, no.1, pp.182–186, Jan. 2024.

[4] J. Rains, J. ur Rehman Kazim, A. Tukmanov, L. Zhang, Q.H. Abbasi, and M.A. Imran, "Practical design considerations for reconfigurable intelligent surfaces," Intelligent Reconfigurable Surfaces (IRS) for Prospective 6G Wireless Networks, Wiley, 2023.

[5] C. Zhang, W. Yi, Y. Liu, K. Yang, and Z. Ding, "Reconfigurable intelligent surfaces aided multi-cell NOMA networks: A stochastic geometry model," IEEE Trans. Commun., vol.70, no.2, pp.951–966, 2022.

[6] M.A. Kishk and M.S. Alouini, "Exploiting randomly located blockages for large-scale deployment of intelligent surfaces," IEEE J. Sel. Areas Commun., vol.39, no.4, pp.1043–1056, 2021.

[7] T. Shafique, H. Tabassum, and E. Hossain, "Stochastic geometry analysis of IRS-assisted downlink cellular networks," IEEE Trans. Commun., vol.70, no.2, pp.1442–1456, 2022.

[8] C. Psomas, H.A. Suraweera, and I. Krikidis, "On the association with intelligent reflecting surfaces in spatially random networks," IEEE International Conference on Communications, pp.1–6, 2021.

[9] Y. Fang, S. Atapattu, H. Inaltekin, and J. Evans, "Optimum reconfigurable intelligent surface selection for wireless networks," IEEE Trans. Commun., vol.70, no.9, pp.6241–6258, 2022.

[10] Y. Wang, C. Chen, H. Zheng, and X. Chu, "Performance of indoor small-cell networks under interior wall penetration losses," IEEE Internet Things J., vol.10, no.12, pp.10907–10915, 2023.

[11] M. Haenggi, Stochastic Geometry for Wireless Networks, Cambridge Univ. Press, 2012.

[12] T. Bai, R. Vaze, and R.W. Heath, "Analysis of blockage effects on urban cellular networks," IEEE Trans. Wireless Commun., vol.13, no.9, pp.5070–5083, 2014.

[13] A.K. Mishra and V. Ponnusamy, "An approximate distribution of estimates of variance components," Biometrics Bulletin, vol.2, no.6, pp.110–114, 1946.

[14] H. Alzer, "On some inequalities for the incomplete gamma function," Math. Comp., vol.66, no.218, p.771–778, 1997.